Molecular Pharmacology Fast Forward. Published on November 24, 2014 as DOI: 10.1124/mol.114.094979
This article has not been copyedited and formatted. The final version may differ from this version.

Modulation of PPARα activity by bile acids causes circadian changes in the intestinal expression of Octn1/*Slc22a4* in mice

Erika Wada, Satoru Koyanagi, Naoki Kusunose, Takahiro Akamine,

Hiroaki Masui, Hana Hashimoto, Naoya Matsunaga, and Shigehiro Ohdo

Department of Pharmaceutics, Faculty of Pharmaceutical Sciences,

Kyushu University, 3-1-1 Maidashi Higashi-ku, Fukuoka 812-8582, Japan

Downloaded from molpharm.aspetjournals.org at ASPET Journals on April 18, 2024

Molecular Pharmacology Fast Forward. Published on November 24, 2014 as DOI: 10.1124/mol.114.094979
This article has not been copyedited and formatted. The final version may differ from this version.

Running title:

Circadian regulation of intestinal expression of Octn1/*Slc22a4*

Correspondence:

Shigehiro Ohdo, Ph.D., Department of Pharmaceutics, Graduate School of Pharmaceutical Sciences, Kyushu University,

3-1-1 Maidashi Higashi-ku, Fukuoka 812-8582, Japan.

Tel.: 81-92-642-6610; Fax: 81-92-642-6614; E-mail: ohdo@phar.kyushu-u.ac.jp

Document information:

Number of text pages, 25

Number of figures, 5

Number of tables, 1

Number of references, 36

Number of words in the Abstract, 248

Number of words in the Introduction, 754

Number of words in the Discussion, 1135

Abbreviations: Octn1, organic cation transporter novel-1; PPARα, peroxisome proliferator-activated receptor-α; *Slc22a4*, soluble carrier protein family 22 member 4; AUC, area under the curve of the serum concentration-time curve; $t_{1/2}$, half-life

Downloaded from molpharm.aspetjournals.org at ASPET Journals on April 18, 2024

Molecular Pharmacology Fast Forward. Published on November 24, 2014 as DOI: 10.1124/mol.114.094979
This article has not been copyedited and formatted. The final version may differ from this version.

Abstract

In addition to their digestive actions, bile acids modulate gene expression by altering the activity of peroxisome proliferator-activated receptor-α (PPARα). The modulatory effects of bile acids have been shown to affect the expression of genes responsible for lipid metabolism as well as membrane transporters. Bile acids are secreted in response to food intake and accumulate in intestinal epithelial cells. In the present study, we identified soluble carrier protein family 22 member 4 (*Slc22a4*), encoding organic cation transporter novel type-1 (Octn1), as a PPARα-regulated gene and its intestinal expression exhibited circadian oscillations in a bile acid-dependent manner. Nocturnally active mice mainly consumed their food around the early dark phase, during which bile acids accumulated in intestinal epithelial cells. PPARα activated the intestinal expression of *Slc22a4* mRNA during the light period, and protein levels of Octn1 peaked before the start of the dark phase. The bile acids that accumulated in intestinal epithelial cells suppressed the PPARα-mediated transactivation of *Slc22a4* in the dark phase. The time-dependent suppression of PPARα-mediated transactivation by bile acids regulated oscillations in the intestinal expression of Octn1/*Slc22a4* during the daily feeding cycle. The results of a pharmacokinetic analysis also revealed that oscillations in the expression of Octn1 caused dosing time-dependent differences in the intestinal absorption of gabapentin (2-[1-(aminomethyl)cyclohexyl]acetic acid). These results suggest a molecular clock-independent mechanism by which bile acid-regulated PPARα activity governs the circadian expression of intestinal organic cation transporters. This mechanism could also account for inter-individual variations in the pharmacokinetics of drugs that are substrates of Octn1.

Downloaded from molpharm.aspetjournals.org at ASPET Journals on April 18, 2024

Molecular Pharmacology Fast Forward. Published on November 24, 2014 as DOI: 10.1124/mol.114.094979
This article has not been copyedited and formatted. The final version may differ from this version.

Introduction

Daily variations in biological functions are thought to affect the efficacy and/or toxicity of drugs; a large number of drugs cannot be expected to have the same potency at different administration time (Lévi, 1996; Hrushesky, 2001; Lis et al., 2003). Dosing time-dependent differences in the therapeutic effects of drugs have been, at least partly, attributed to circadian-related changes in drug disposition, for example, absorption, distribution, metabolism, and elimination (Ohdo, 2007). The small intestine is an important organ for the absorption of a drug following its oral administration, and various types of transporters are expressed on intestinal epithelial cells (Tsuji and Tamai, 1996; Bleasby, 2006; Stearns et al., 2008). Recent studies reported that the mRNA levels of intestinal transporters exhibited 24-h oscillations (Murakami et al., 2008; Stearns et al., 2008; Hamdan et al., 2012), which could account for dosing time-dependent changes in the absorption of drugs. However, a systematic analysis of the circadian regulation of intestinal transporters has not yet been conducted.

In mammals, 24-h rhythms in various biological processes are under the control of a molecular pacemaker consisting of circadian clock genes (Gekakis et al., 1998; Kume et al., 1999; Yoo et al., 2005). These gene products constitute an oscillatory mechanism that is based on self-sustained transcriptional/translational feedback loops (Gekakis et al., 1998; King et al., 1997). *Clock* was the first circadian clock gene to be identified in mammals. The *Clock* gene encodes the transcription factor, CLOCK protein, which dimerizes with BMAL to activate the transcription of *Period* (*Per*) and *Cryptochrome* (*Cry*) genes through E-box or E-box-like enhancer sequences (Gekakis et al., 1998; Preitner et al., 2002; Yoo et al., 2005). Once PER and CRY proteins have reached a critical concentration, they

Downloaded from molpharm.aspetjournals.org at ASPET Journals on April 18, 2024

Molecular Pharmacology Fast Forward. Published on November 24, 2014 as DOI: 10.1124/mol.114.094979
This article has not been copyedited and formatted. The final version may differ from this version.

attenuate the transactivation of CLOCK/BMAL1, thereby generating circadian oscillations in their own transcription (Gekakis et al., 1998; Yoo et al., 2005). CLOCK/BMAL, PER, and CRY proteins also regulate the expression of the orphan nuclear receptor REV-ERBα, which, in turn, represses the transcription of *Bmal* (Preitner et al., 2002). This mechanism interconnects the positive and negative limbs of the circadian clockwork circuitry and also regulates 24-h variations in output physiology through the periodic activation/repression of clock-controlled output genes (Jin et al., 1999; Maemura et al., 2000; Oishi et al., 2003). Proline- and acid-rich basic leucine zipper proteins, hepatic leukemia factor, thyrotroph embryonic factor, and D-site binding protein are examples of such output mediators because their expression is regulated by core oscillator components (Ripperger et al., 2000). The circadian-controlled output pathways include those that control the expression of many enzymes and regulators involved in xenobiotic detoxification, such as cytochrome P450 enzymes, carboxylesterases, and xenobiotic transporters (Gachon et al., 2006).

In addition to the intracellular molecular clock, circadian rhythms in cell physiology are also generated by extracellular factors (Balsalobre et al., 2000a, 2000b; (Oishi et al., 2005; Terazono et al., 2003). After the intake of food, bile acids are secreted into the lumen of the small intestine, in which they act not only as a digestive detergent of lipids, but also as a modulator of gene expression in epithelial cells (Sinal et al., 2001). When food is plentiful, nocturnally active mice ingest most of their food during the dark phase (Ritskes-Hoitinga, 2004). In a recent study, we found that bile acids time-dependently accumulated in the intestinal epithelial cells of mice during their daily feeding cycle (Okamura et al., 2014). This time-dependent accumulation of bile acids

Downloaded from molpharm.aspetjournals.org at ASPET Journals on April 18, 2024

Molecular Pharmacology Fast Forward. Published on November 24, 2014 as DOI: 10.1124/mol.114.094979
This article has not been copyedited and formatted. The final version may differ from this version.

generated circadian changes in the intestinal expression of peptide absorption transporter PepT1 through the periodic suppression of peroxisome proliferator-activated receptor-α (PPARα)-mediated transactivation (Okamura et al., 2014)

PPARα is a ligand-activated transcription factor that belongs to the nuclear-hormone receptor superfamily (Issemann and Green, 1990; Bookout et al., 2006). PPARα is highly expressed in the liver, heart, kidney, brown adipose tissue, muscle, and small intestine of mammals (Braissant et al., 1996). Numerous studies using PPARα-null mice demonstrated that this nuclear receptor has critical roles in energy metabolism, hepatic steatosis, inflammation, cardiac pathophysiology, cell-cycle regulation, and oncogenesis (Lee et al., 2002; Lefebvre et al., 2006). In the present study, we screened PPARα-regulated genes whose intestinal expression was dependent on bile acids. DNA microarray analyses using RNA isolated from the intestinal epithelial cells of mice revealed that 58 genes were regulated by PPARα in a bile acid-dependent manner. Among these, the expression of the soluble carrier protein family 22 member 4 (*Slc22a4*) gene, encoding organic cation transporter novel type-1 (Octn1), exhibited significant circadian oscillations. Therefore, we focused on this gene in order to investigate how time-dependent oscillations in the intestinal expression of Octn1 affected the pharmacokinetics of its typical substrate.

Materials and methods

Animals and treatment

Male PPARα-null mice (129S4-Svjae-PPARαmuGonzN12) with a JcI:ICR background and male wild-type mice of the same strain were housed in a temperature-controlled (24 ±

Downloaded from molpharm.aspetjournals.org at ASPET Journals on April 18, 2024

Molecular Pharmacology Fast Forward. Published on November 24, 2014 as DOI: 10.1124/mol.114.094979
This article has not been copyedited and formatted. The final version may differ from this version.

1°C) room under a 12 h light: 12 h dark cycle. Under the light/dark cycle, zeitgeber time (ZT) 0 was designated as lights on and ZT12 as lights off. Mice were fed *ad libitum* at least 2 weeks before the experiments. Animals were treated in accordance with the guidelines stipulated by the Animal Care and Use Committee of Kyushu University. Gabapentin (2-[1-(aminomethyl)cyclohexyl]acetic acid; Tokyo Chemical Industry Co. Ltd., Tokyo, Japan) was dissolved in water and administered orally at 65 mg/kg body weight.

Microarray Analysis.

We performed oligonucleotide microarray analyses using RNA isolated from the intestinal epithelial cells of wild-type and PPARα-null mice in order to determine which PPARα-regulated genes were expressed in a bile acid-dependent manner. The proximal segments of the jejunum were isolated from mice at ZT12 when nocturnally active animals started daily feeding, and were then flushed with ice-cold saline. These segments were preincubated for 15 minutes at 37°C in Krebs-Ringer buffer (128.9 mM NaCl/ 4.2 mM KCl/ 1.5 mM $CaCl_2$/ 22.4 mM $NaHCO_3$/ 1.2 mM KH_2PO_4/ 1.3 mM $MgSO_4$/ 10 mM D-glucose), and equilibrated with 95% O_2 and 5% CO_2. After the preincubation, CA was added to the buffer to give a final concentration of 500 μM, and the segments were incubated at 37°C for 2 h. The concentration of CA is enough to suppress the expression of PPARα-target gene in small intestine of mice (Okamura et al., 2014). To vehicle control groups, dimethyl sulfoxide (DMSO) and ethanol were added to give final concentration of 0.05% and 0.25%, respectively. After the incubation, total RNA (250 ng) was extracted from the epithelial cells of intestinal segments using RNAiso (Takara Bio Inc., Otsu, Japan). The quality of the extracted RNA was analyzed using an Agilent 2100 Bioanalyzer (Agilent

Downloaded from molpharm.aspetjournals.org at ASPET Journals on April 18, 2024

Molecular Pharmacology Fast Forward. Published on November 24, 2014 as DOI: 10.1124/mol.114.094979
This article has not been copyedited and formatted. The final version may differ from this version.

Technologies, Santa Clara, CA). cRNA was amplified and labeled using a low input quick amp labeling kit. Labeled cRNA was hybridized to a 44K Agilent 60-mer oligomicroarray (Whole Mouse Genome Microarray kit version 2.0) according to the manufacturer's instructions. All hybridized microarray slides were washed and scanned using an Agilent scanner. Relative hybridization intensities and background hybridization values were calculated using Agilent Feature Extraction software (version 9.5.1.1). Raw signal intensities and flags for each probe were calculated from hybridization intensities and spot information according to the procedures recommended by Agilent. The raw signal intensities of two samples were log2-transformed and normalized by a quantile algorithm in the "preprocessCore" library package of the Bioconductor software. This produced a gene expression matrix consisting of 55,681 probe sets, and differentially expressed genes between samples were selected by calculating Z-scores and ratios (non-log scaled fold-change) as follows: for up-regulated genes: a Z-score of 2.0 or more and a ratio of 2-fold or more; and for down-regulated genes: a Z-score of -2.0 or less and a ratio of 0.5 or less. We used three criteria to identify putative bile acid-dependent PPARα-regulated genes: 1) Wild-type (vehicle) > PPARα-null (vehicle); 2) Wild-type (vehicle) > Wild-type (CA); and 3) PPARα-null (vehicle) ≒ PPARα-null (CA). Microarray data were submitted to the Gene Expression Omnibus at the National Center for Biotechnology Information (accession # GSE55443).

RNA extraction and quantitative RT-PCR analysis

RNA was extracted using RNAiso reagent (Takara). cDNA was synthesized using a ReverTra Ace® qPCR RT Kit (Toyobo) and amplified by PCR. Real-time PCR analysis

Downloaded from molpharm.aspetjournals.org at ASPET Journals on April 18, 2024

Molecular Pharmacology Fast Forward. Published on November 24, 2014 as DOI: 10.1124/mol.114.094979
This article has not been copyedited and formatted. The final version may differ from this version.

was performed on diluted cDNA samples using THUNDERBIRDTM SYBR® qPCR Mix (Toyobo) with the 7500 Real-time PCR system (Applied Biosystems). Data were normalized using actin mRNA as a control because its intestinal expression was constant throughout the day. The sequences of mouse *Slc22a4* primers were as follows: 5'-CCTGTTCTGTGTTCCCCTGT-3' and 5'-GGTTATGGTGGCAATGTTCC-3'. The sequences of mouse *Actin* primers (internal control) were as follows: 5'-CACACCTTCTACAATGAGCTGC-3' and 5'-CATGATCTGGGTCATCTTTTCA-3'. The sequences of human *SLC22A4* primers were as follows: 5'-CCAGAAACCTTAGAGCAGATGCAGA-3' and 5'-GTCAGTCCATTTCAGCGGGA-ACA-3'. The sequences of human *ACTIN* primers (internal control) were as follows: 5'-AGAGCTACGAGCTGCCTGAC-3' and 5'- AGCACTGTGTTGGCGTACAG-3'.

Cells and treatment

Immortalized small intestine epithelial cells (aMoS7), established from adult murine intestinal crypts, were kindly provided by Dr. Totsuka (Tokyo University). The human colon carcinoma cell line, Caco-2, was obtained from the American Type Culture Collection. These cells were maintained in Dulbecco's modified Eagle's medium (DMEM; Sigma Aldrich) supplemented with 10% fetal bovine serum (FBS; SIGMA Aldrich), 25 U/mL of penicillin (GIBCO), 25 μg/mL of streptomycin (GIBCO), and 10 μg/mL of insulin (Wako, Osaka, Japan). For luciferase reporter assay, aMoS7 were transfected with reporter and expression vectors encoding PPARα and its dimerization partner retinoid X receptor α (RXRα) using Lipofectamine-LTX reagent (Invitrogen). Variations in transfection

Downloaded from molpharm.aspetjournals.org at ASPET Journals on April 18, 2024

Molecular Pharmacology Fast Forward. Published on November 24, 2014 as DOI: 10.1124/mol.114.094979
This article has not been copyedited and formatted. The final version may differ from this version.

efficiency were corrected by co-transfecting cells with 0.5 ng of pGL4.74 [hRluc/TK] (Promega). The total amount of DNA per well was adjusted by adding the pcDNA3.1 vector (Invitrogen). To investigate the influence of PPARα and RXRα on the mRNA levels of *Slc22a4*, aMoS7 or Caco-2 cells were seeded on 24-well plates and then transfected with vectors encoding PPARα and RXRα as described above. Total RNA was extracted from cells 24 h after transfection. To synchronize the circadian clocks in cultured aMoS7 cells, serum shock was performed as follows: cells were grown to semi-confluence in DMEM supplemented with 5% FBS. On the day of serum shock, 50% FBS was added for 2 h and cells were then incubated in DMEM supplemented with 1% FBS. Cells were harvested for RNA extraction at the indicated times after the serum treatment. aMoS7 cells were also treated with 500 μM cholic acid (CA; Wako), the main composition of bile acids in mice (Okamura et al., 2014), for the indicated times.

Construction of luciferase reporter vectors

The 5'-flanking region of the mouse *Slc22a4* gene (from -1064 bp to +33; +1 indicates the transcription start site) was amplified using Platinum® PCR SuperMix High Fidelity (Invitrogen) using the forward primer 5'-CCCGGTTTGTGCAAAGTGTT-3' and reverse primer 5'-CTTCCTAGGTGGCTGCGTG-3'. The PCR products were purified and ligated into pGL4.12 promoter vector (Promega). Two putative PPREs on *Slc22a4*-Luc were mutated in combination with others, using a QuickChange Site-Directed mutagenesis kit (Stratagene, San Diego, CA). The changed sequences were as follows: base pairs (bp) of

Downloaded from molpharm.aspetjournals.org at ASPET Journals on April 18, 2024

Molecular Pharmacology Fast Forward. Published on November 24, 2014 as DOI: 10.1124/mol.114.094979
This article has not been copyedited and formatted. The final version may differ from this version.

–847 to –835 were changed from TCCCTTCCTCCCT to TCCAGATCTTCCT, and bp of –653 to –640 were changed from AGGCCACAGGGAA to AGGCCTCGAGGAA

.

Luciferase reporter assay

At 24 h after transfection of cells with reporters and expression constructs, cells were harvested, and the cell lysate was analyzed using a dual-luciferase reporter assay system (Promega). The ratio of firefly luciferase activity (expressed from reporter construct) to Renilla luciferase activity (expressed from pRL-TK) in each sample served as a measure of normalized luciferase activity.

Western blotting

Cell membrane fractions or nuclear extractions from epithelial cells of mouse small intestine were prepared at six time points as described previously (Murakami et al., 2008). Then, 20 μg of total protein lysates was resolved by 8 or 10% SDS-PAGE, transferred to a PVDF membrane, and probed with rat monoclonal antibodies against PPARα (Santa Cruz Biotechnology), Octn1 (Alpha Diagnostic International) or Actin (Santa Cruz Biotechnology). Specific antigen-antibody complexes were visualized using horseradish peroxidase-conjugated secondary antibodies and Chemi-Lumi One (Nacalai Tesque).

Down-regulation of Octn1

We designed small interfering RNA (siRNA) for knockdown experiments using the BLOCK-iTTM RNAi Designer (https://rnaidesigner.invitrogen.com/rnaiexpress/). The

Downloaded from molpharm.aspetjournals.org at ASPET Journals on April 18, 2024

Molecular Pharmacology Fast Forward. Published on November 24, 2014 as DOI: 10.1124/mol.114.094979
This article has not been copyedited and formatted. The final version may differ from this version.

target sequence of mouse *Slc22a4* was as follows; GUUGGUACCGACACGUCUGACCUAA (GenBank accession No. NM_019687). The oligonucleotides were transfected into aMoS7 cells at a final concentration of 10, 50, or 100 pmol/well using Lipofectamine 2000 reagent (Invitrogen). The total amount of siRNA per well was adjusted by adding control siRNA. Down-regulation of Octn1 was confirmed by Western blotting.

Determination of gabapentin incorporation into aMoS7 cells

aMoS7 cells were preincubated for 30 min at 37˚C with 480 μL of Krebs-Ringer buffer and equilibrated with 95% O_2, 5% CO_2. After the preincubation, [^{3}H]-gabapentin (Muromachi Chemical Inc., Tokyo, Japan) was added to the incubation medium to give a final concentration at 10 nM, and the cells were incubated for 30 min at 37˚C. After the incubation, the cells were rinsed with ice-cold PBS twice. Thereafter, cells were homogenized in PBS. The radioactivity in each fraction was determined using a liquid scintillation counter after sufficient solubilization. The amounts of [^{3}H]-gabapentin incorporated into the aMoS7 cells were expressed as pmol/ mg protein/min.

Determination of intestinal accumulation of gabapentin.

Proximal segments of the jejunum were isolated from wild-type mice at ZT2 and ZT14. The isolated intestinal segments were flushed with ice-cold saline and preincubated at 37°C for 20 min in Krebs-ringer buffer. After the preincubation, [^{3}H]-gabapentin was added to the incubation buffer at a final concentration of 5 μM, and the segments were incubated at 37°C for 30 min in the presence or absence of 10 mM tetraethylammonium

Downloaded from molpharm.aspetjournals.org at ASPET Journals on April 18, 2024

Molecular Pharmacology Fast Forward. Published on November 24, 2014 as DOI: 10.1124/mol.114.094979
This article has not been copyedited and formatted. The final version may differ from this version.

(TEA) and 100 μM non-radio-labeled (cold) gabapentin. After the incubation, each segment was rinsed with ice-cold PBS 3 times and homogenized in 300 μL PBS. Radioactivity in the homogenate was determined using a liquid scintillation counter after sufficient solubilization. The intestinal accumulation of [^{3}H]- gabapentin was expressed as pmol/mg protein/min.

Measurement of gabapentin concentrations in serum

Serum concentrations of gabapentin were measured by high performance liquid chromatography using DL-norvaline as an internal standard. Gabapentin and DL-norvaline were derivatized with o-phthaldialdehyde. The mobile phase of phosphate buffer (pH 3.0; 20 mM)-acetonitrile (4:3, v/v) was eluted at 1.0 mL/min through a 5C$_{18}$-MS-II column (4.6 × 150 mm; Nacalai Tesque) using an LC-20AD pump (Shimadzu). The separated analyte was detected using the Spectrofluorometric Detector RF-550 (excitation and emission at 330 and 450 nm, respectively; Shimadzu). The total run time was 30 min with DL-norvaline and gabapentin retention times of 7 and 15 min, respectively.

Pharmacokinetic analysis

Serum concentrations of gabapentin were analyzed using the nonlinear mixed effect model (NONMEM) program. NONMEM is a computer program designed to analyze pharmacokinetics in study populations by pooling data. Population pharmacokinetic parameters were calculated using 39 serum gabapentin concentrations obtained from 39 mice following the one-compartment model with first-order absorption (the PREDPP program, subroutines ADVAN2 and TRANS2). Bayesian estimates of individual

Downloaded from molpharm.aspetjournals.org at ASPET Journals on April 18, 2024

Molecular Pharmacology Fast Forward. Published on November 24, 2014 as DOI: 10.1124/mol.114.094979
This article has not been copyedited and formatted. The final version may differ from this version.

pharmacokinetic parameters were obtained by the post hoc method of the NONMEM program. The improvement in fit obtained with the addition of a covariate was assessed by changes in the objective function (OBJ). At the assessing step, the OBJ values were compared between each model. A difference in -2 L.L.D was asymptotically distributed as $\chi 2$ with degrees of freedom equal to the number of parameters. A difference of 3.841 in the value of OBJ with freedom 1 was accepted as significant ($p<0.05$).

Statistical analysis

The significance of differences between groups was validated by the Bonferroni test for multiple comparisons. The 5% level of probability was considered to be significant for the Bonferroni test. The Student's *t*-test was used for comparisons between two groups. The 1% level of probability was considered to be significant for the Student's *t*-test.

Results

Screening for PPARα-regulated genes whose expression is dependent on bile acids.

Bile acids repress PPARα-mediated expression of its target genes without changing the PPARα binding to the DNA response elements (Sinal et al., 2001). Since bile acids interfere with the recruitment of CBP/p300 to the PPARα/RXRα complexes, it is possible that the intestinal expression of a variety of PPARα-regulated genes is also modulated by bile acids. To screen PPARα-regulated genes whose intestinal expression is repressed by bile acids, we performed oligonucleotide microarray analyses using RNA isolated from the CA-treated intestinal cells of wild-type or PPARα-null mice. Three criteria were used to select bile acid-dependent PPARα-regulated genes (see Materials and methods**)**. We identified 58 genes that were candidates for PPARα-regulated genes whose expression was

Downloaded from molpharm.aspetjournals.org at ASPET Journals on April 18, 2024

Molecular Pharmacology Fast Forward. Published on November 24, 2014 as DOI: 10.1124/mol.114.094979
This article has not been copyedited and formatted. The final version may differ from this version.

suppressed by bile acids (**Supplemental Table S1)**. They included 7 genes that encoded lipid metabolism-related proteins. Known PPARα-target genes such as acyl CoA oxidase, fatty acid translocase (CD36), and apolipoprotein A-II were identified among the 7 genes (Dreyer et al., 1992; Vu-Dac et al., 1995; Motojima et al., 1998). On the other hand, 12 genes encoding plasma-membrane transporters were also screened as bile acid-dependent PPARα-regulated genes (**Fig. 1A**). Of these, the mouse *Slc22a4* gene contained several PPAR response elements (PPREs) in its promoter region (**Fig. 1B**). The results of luciferase reporter analysis revealed that the PPREs in the mouse *Slc22a4* gene were responsible for the PPARα/RXRα-mediated transactivation (**Fig. 1B**). The mRNA levels of *Slc22a4* in the cultured mouse intestinal cells, aMoS7, were significantly increased by the transfection of PPARα and RXRα (**Fig. 1C left**). Consistent with studies showing bile acid represses PPARα activity, the PPARα/RXRα-induced expression of *Slc22a4* was suppressed by the CA treatment. A similar putative PPRE was also located in the promoter region of the human *SLC22A4* gene. As shown in **Fig. 1C (**right panel), the repressing effect of CA on the PPARα/RXRα-induced expression of *SLC22A4* was observed in the human colon carcinoma cell line, Caco-2, which is often used as an *in vitro* model of the intestinal system.

Bile acid-regulated PPARα activity was responsible for the time-dependent expression of *Slc22a4* in intestinal epithelial cells.

As reported previously (Ritskes-Hoitinga, 2004), wild-type mice consumed ~80% of their food during the dark phase when they were fed *ad libitum* (**Fig. 2A**). The amount of bile acids in the intestinal epithelial cells of wild-type mice exhibited obvious circadian oscillations, with higher levels being observed during the dark phase (**Fig. 2B**). PPARα-null also showed the obvious circadian accumulation of bile acids; however, no significant

Downloaded from molpharm.aspetjournals.org at ASPET Journals on April 18, 2024

Molecular Pharmacology Fast Forward. Published on November 24, 2014 as DOI: 10.1124/mol.114.094979
This article has not been copyedited and formatted. The final version may differ from this version.

differences were observed in the temporal pattern of food intake and intestinal bile acid accumulation between PPARα-null and wild-type mice (**Fig. 2A and B**). These results suggested that the secretory function of bile acids in response to food intake in PPARα-null mice may not be PPARα-dependent.

A significant circadian oscillation in *Slc22a4* mRNA levels was observed in the small intestine of wild-type mice under the *ad libitum* feeding condition ($p<0.05$, **Fig. 2C**); mRNA levels increased during the light phase and then decreased after the start of the dark phase. The oscillation in the expression of *Slc22a4* mRNA was nearly the anti-phase to that in bile acid accumulation. The expression of PPARα protein in the intestinal epithelial cells in wild-type mice was detected at all examined time points, although the protein levels were not obviously oscillated in a circadian time-dependent manner (**Fig. 2D**). By contract, the protein levels of Octn1 oscillated in a circadian time-dependent manner. They peaked before the start of the dark phase (**Fig. 2D**). The deletion of PPARα had a negligible effect on oscillations in bile acid accumulation in intestinal epithelial cells, but the amplitude of the rhythms in *Slc22a4* mRNA and the Octn1 protein decreased in PPARα-null mice (**Fig. 2C and D**). These results suggest that PPARα acts as a positive regulator of *Slc22a4* expression in intestinal epithelial cells. The PPARα-mediated expression of *Slc22a4* appeared to be repressed by bile acids during the dark phase.

Temporal exposure of intestinal epithelial cells to bile acids causes an oscillation in *Slc22a4* mRNA expression.

The oscillations observed in the intestinal accumulation of bile acids in wild-type mice were anti-phase to the *Slc22a4* mRNA rhythm. To investigate whether the cyclic exposure of intestinal epithelial cells to bile acids resulted in the generation of *Slc22a4* mRNA oscillations, we examined the temporal expression profile of *Slc22a4* mRNA in

Downloaded from molpharm.aspetjournals.org at ASPET Journals on April 18, 2024

Molecular Pharmacology Fast Forward. Published on November 24, 2014 as DOI: 10.1124/mol.114.094979
This article has not been copyedited and formatted. The final version may differ from this version.

cultured intestinal epithelial cells during repetitive treatments with CA. In this experiment, we also set comparative cells whose circadian clock was synchronized by a treatment with 50% serum (Balsalobre et al., 2000a). The exposure of aMoS7 to 50% serum for 2 h resulted in the circadian expression of *Per1* and *Per2* (**Fig. 3A upper**). The circadian expression of *Per1* and *Per2* persisted for up to 48 h after the serum treatment. In contrast, *Slc22a4* mRNA levels transiently increased after the serum treatment; however, a persistent circadian oscillation was not detected in mRNA expression levels (**Fig. 3A lower**). The treatment of aMoS7 cells with 500 μM CA for 4 h caused a significant decrease in *Slc22a4* mRNA levels ($p<0.05$, **Fig. 3B lower**), whereas mRNA levels gradually increased after the removal of CA from the medium. The restored *Slc22a4* mRNA levels were also suppressed by the treatment of cells with 500 μM CA. However, the repetitive treatment of cells with CA had a negligible effect on the expression of *Per1* and *Per2* (**Fig. 3B upper**). These results further supported the notion that oscillations in the intestinal expression of *Slc22a4* mRNA is dependent on the cyclic accumulation of bile acids.

Influence of down-regulation of *Slc22a4* on the uptake of gabapentin into aMoS7 cells.

A previous study demonstrated that genetic polymorphisms in the human *SLC22A4* gene affected the pharmacokinetics of gabapentin (Urban et al., 2007). Consequently, gabapentin was considered to be an attractive candidate as a substrate for Octn1; however, there is no direct evidence for the contribution of Octn1 to the transport of gabapentin. Therefore, we investigated whether Octn1 mediated the incorporation of gabapentin into intestinal epithelial cells. The treatment of aMoS7 cells with 500 μM CA for 4 h transiently decreased the protein levels of Octn1 (**Fig. 4A**). The incorporation of gabapentin into intestinal epithelial cells was decreased in parallel with Octn1 protein levels. Gabapentin incorporation was re-elevated according to an increase in Octn1 protein levels, implying

Downloaded from molpharm.aspetjournals.org at ASPET Journals on April 18, 2024

Molecular Pharmacology Fast Forward. Published on November 24, 2014 as DOI: 10.1124/mol.114.094979
This article has not been copyedited and formatted. The final version may differ from this version.

that abundance of Octn1 protein in the intestinal epithelial cells is correlated with its transport activity. The transfection of aMoS7 cells with siRNA against *Slc22a4* reduced Octn1 protein levels (**Fig. 4B**). The transfection of siRNA dose-dependently decreased the incorporation of gabapentin into aMoS7 cells. These results indicated that Octn1 contributed to the incorporation of gabapentin into cultured mouse intestinal epithelial cells.

Influence of dosing times on gabapentin pharmacokinetics.

Since the intestinal expression of Octn1 oscillated in a time-dependent manner in wild-type mice (**Fig. 2D**), we determined whether this oscillation affected the pharmacokinetics of gabapentin. After incubation of jejunal segments with 5μM [^{3}H]-gabapentin, accumulation of the radio-rebelled compound in the epithelial cells showed a significant time-dependent variation (**Fig. 5A**). The amount of [^{3}H]-gabapentin incorporation was significantly higher at ZT14 than at ZT2 ($p<0.05$). The intestinal accumulation of [^{3}H]-gabapentin was suppressed when the segments were incubated in the presence of 10 mM TEA, a typical substrate of Octn1 (Tamai et al., 2000), but the accumulation was still higher at ZT14 than at ZT2. Furthermore, the time-dependent difference in the intestinal accumulation of [^{3}H]-gabapentin was disappeared by incubating the segments with both 10 mM TEA and 100 μM non-radio-labeled (cold) gabapentin.

Serum concentrations peaked 0.5 h after the oral administration of gabapentin (65 mg/kg body weight) (**Fig. 5B**), while a significant dosing time-dependent difference was observed in the maximum serum concentrations (C_{max}) of gabapentin (**Fig. 5B**). Serum gabapentin concentrations 0.5 h after the drug injection at ZT14 were significantly higher than those after the injection at ZT2 ($p<0.05$). The pharmacokinetics of gabapentin were analyzed using 39 serum concentrations obtained from 39 mice. The final model derived from all data was as follows: CL/F (L/h/kg) = 2.22, Vd (L/kg) = 0.758, and ka (h^{-1}) =0.948

Downloaded from molpharm.aspetjournals.org at ASPET Journals on April 18, 2024

Molecular Pharmacology Fast Forward. Published on November 24, 2014 as DOI: 10.1124/mol.114.094979
This article has not been copyedited and formatted. The final version may differ from this version.

 2.05^{DT}, where CL is the apparent clearance, Vd is the apparent volumes of distribution, and ka is the absorption rate constant. DT represented the dosing time: DT = 0 if the injection of the drug was at ZT2; DT = 1 if the injection of the drug was at ZT14. Using population parameters, individual pharmacokinetic parameters were also calculated based on Bayesian estimates, and the area under the curve of the serum concentration-time curve (AUC) and half-life ($t_{1/2}$) were then derived from them (**Table 1**). The value of ka was significantly larger in mice administered gabapentin at ZT14 than at ZT2 ($p<0.01$), whereas no significant dosing time-dependent difference was observed in the other pharmacokinetic parameters of gabapentin.

Discussion

Circadian rhythms in various biological processes are considered to be driven by an internal timekeeping system consisting of clock genes, whereas several rhythms observed in cell physiology are also generated by stimulations from extracellular signals. When food moves through the gastrointestinal tract, bile juices are secreted into the small intestine, in which they act not only as a digestive detergent of lipids, but also as a modulator of gene expression in epithelial cells. Under the *ad libitum* feeding condition, nocturnally active mice ingested most of their food during the dark phase, during which bile acids accumulated in intestinal epithelial cells. The present study showed that the time-dependent accumulation of bile acids caused oscillations in the intestinal expression of *Slc22a4*/Octn1 through the periodic suppression of PPARα-mediated transactivation.

PPARα activates the transcription of its target genes by binding to PPREs. A computer-aided analysis of the mouse *Slc22a4* promoter region identified several putative

Downloaded from molpharm.aspetjournals.org at ASPET Journals on April 18, 2024

Molecular Pharmacology Fast Forward. Published on November 24, 2014 as DOI: 10.1124/mol.114.094979
This article has not been copyedited and formatted. The final version may differ from this version.

sequences resembling PPRE. In fact, the response elements located bp from –847 to –835 and bp from –653 to –640 were responsible for the PPARα-mediated transactivation of the *Slc22a4* gene. As PPARα was constantly expressed throughout the day in the epithelial cells of small intestine, bile acid-induced repression of *Slc22a4* was unlikely associated with a decrease in the PPARα abundance. A previous study demonstrated that bile acids repressed the expression of PPARα-regulated genes by interfering with the recruitment of the co-transcriptional activator CBP/p300 (Sinal et al., 2001). The repressive action of bile acids may also be applicable to the PPARα-mediated transactivation of the *Slc22a4* gene.

Circadian gene expression is caused not only by a cell-autonomous mechanism but also by time-dependent changes in extracellular stimuli (Oishi et al., 2005; Terazono et al., 2003). Such rhythmic expression of these genes is also observed in cultured cells after brief treatment with various compounds (Balsalobre et al., 2000a, 2000b); therefore, the peripheral oscillator in cultured cells is used as an *in-vitro* model for the circadian clock. Although treatment of aMoS7 cells with high concentration serum induced the oscillation in the mRNA expression of *Per1* and *Per2* with a period length of about 24 h, no significant circadian expression of *Slc22a4* mRNA was detected in the serum-treated cells. By contrast, the repetitive treatment of aMoS7 cells with CA decreased and increased the mRNA levels of *Slc22a4* without affecting the expression of *Per1* and *Per2*. These findings suggest that oscillation in the intestinal expression of *Slc22a4* is not driven by cell-autonomous mechanism. The cyclic accumulation of bile acids in the intestinal epithelial cells appears to cause circadian expression of *Slc22a4.*

The expression of Octn1/*Slc22a4* has not only been detected in the small intestine, but also in the kidney and adipose tissues (Bleasby et al., 2006). Three types of Octn

Downloaded from molpharm.aspetjournals.org at ASPET Journals on April 18, 2024

Molecular Pharmacology Fast Forward. Published on November 24, 2014 as DOI: 10.1124/mol.114.094979
This article has not been copyedited and formatted. The final version may differ from this version.

transporters have been identified in mice (Tamai et al., 1997; Wu et al., 1998; Tamai et al., 2000). Both Octn1 and Octn2 transport carnitine and tetraethylammonium (TEA), whereas Octn1 selectively transports TEA (Tamai et al., 2000). Genetic polymorphisms in the human *SLC22A4* gene were found to be relevant to inter-individual differences in the pharmacokinetics of gabapentin (Urban et al., 2007). Therefore, OCTN1 is considered to be responsible for the membrane transportation of gabapentin. However, direct evidence has not yet been produced to confirm whether the intestinal absorption of gabapentin is dependent on Octn1. As a result of experiments using cultured mouse intestinal epithelial cells, the protein levels of Octn1 were decreased and increased after transient treatment with CA. The fluctuation of Octn1 was paralleled with that of gabapentin incorporation. Furthermore, incorporation of gabapentin into aMoS7 cells was also decreased by the down-regulation of Octn1. These findings suggest that the organic cation transporter is capable of incorporating gabapentin into mouse intestinal epithelial cells. The ability of Octn1 to transport gabapentin was also confirmed by the fact that accumulation of [^{3}H]-gabapentin into the intestinal segments was suppressed when segments were incubated with both gabapentin and typical Octn1's substrate TEA. However, the intestinal accumulation of [^{3}H]-gabapentin was still higher at ZT14 than at ZT2, suggesting that a second transporter mediates uptake and that the activity of second transporter also oscillated in a circadian-dependent manner. This notion was also supported by the fact that the time-dependent difference in the intestinal accumulation of [^{3}H]-gabapentin was disappeared by incubating the segments with both TEA and excessive amount of non-radio-labeled gabapentin. Another type of bile acid-dependent PPARα target transporter may also contribute to uptake of gabapentin into the intestinal epithelial cells.

Under the *ad libitum* feeding condition, Octn1 protein levels in the small intestines

Downloaded from molpharm.aspetjournals.org at ASPET Journals on April 18, 2024

Molecular Pharmacology Fast Forward. Published on November 24, 2014 as DOI: 10.1124/mol.114.094979
This article has not been copyedited and formatted. The final version may differ from this version.

of mice were increased during the dark phase. Oscillations in the levels of the Octn1 protein were delayed by approximately 8 h relative to its mRNA rhythm. This delay in the expression of Octn1 in the membrane fraction of intestinal epithelial cells may have been due to the kinetics of protein synthesis or membrane transportation. The maximum serum concentrations (C_{max}) of gabapentin after the injection of the drug at the dark phase (ZT14) were significantly higher than those after the same injection at the light phase (ZT2). Higher concentrations of gabapentin coincided with increases in the intestinal expression of Octn1. The contribution of Octn1 to dosing time-dependent changes in the absorption of gabapentin was also supported by the pharmacokinetic analysis using the NONMEM program. In this analysis, we determined the pharmacokinetic parameters following the one-compartment model with first-order absorption. The dosing time-dependent difference in the serum concentrations of gabapentin was attributed to circadian changes in the absorption rate constant (ka). These results indicate that circadian oscillations in the intestinal expression of Octn1 may have caused the time-dependent change in the absorption process of gabapentin. Only a few compounds have so far been identified as Octn1 substrates. An increase in the intestinal expression of Octn1 during the feeding time may also contribute to enhancements in the absorption of some nutrients.

The individualization of pharmacotherapy has mainly been achieved by monitoring drug concentrations. Consequently, dosage adjustments have been based on inter-individual differences in drug pharmacokinetics; however, intra- as well as inter-individual variabilities should be considered in order to further improve rational pharmacotherapy because the pharmacokinetics of many drugs also vary depending on

Downloaded from molpharm.aspetjournals.org at ASPET Journals on April 18, 2024

Molecular Pharmacology Fast Forward. Published on November 24, 2014 as DOI: 10.1124/mol.114.094979
This article has not been copyedited and formatted. The final version may differ from this version.

circadian changes in each process including absorption, distribution, metabolism, and excretion (Ohdo et al., 2007). In the present study, we found a molecular clock-independent mechanism by which bile acid-regulated PPARα activity governed the circadian expression of Octn1/*Slc22a4* in the small intestines of mice. A microarray analysis revealed that several types of PPARα target genes encoding membrane transporters were expressed in a bile acid-dependent manner. Consequently, the intestinal expression of these membrane transporters may also exhibit circadian oscillations that are driven by time-dependent interactions between bile acids and PPARα. Hereafter, we should systematize the circadian regulation mechanism underlying transporter functions, and make a strategic arrangement to predict the absorption of a drug after its oral administration.

Downloaded from molpharm.aspetjournals.org at ASPET Journals on April 18, 2024

Molecular Pharmacology Fast Forward. Published on November 24, 2014 as DOI: 10.1124/mol.114.094979
This article has not been copyedited and formatted. The final version may differ from this version.

Acknowledgments

The authors thank the technical support for measurement of platinum from the Center of Advanced Instrumental Analysis, Kyushu University.

Downloaded from molpharm.aspetjournals.org at ASPET Journals on April 18, 2024

Molecular Pharmacology Fast Forward. Published on November 24, 2014 as DOI: 10.1124/mol.114.094979
This article has not been copyedited and formatted. The final version may differ from this version.

Authorship Contributions

Participated in research design: Wada, Koyanagi, and Ohdo.

Conducted experiments: Wada, Koyanagi, Kusunose, and Akamine.

Contributed new reagents or analytic tools: Wada, and Matusnaga.

Performed data analysis: Wada, Koyanagi, Masui, and Hashimoto.

Wrote or contributed to the writing of the manuscript: Wada, Koyanagi, and Ohdo.

Downloaded from molpharm.aspetjournals.org at ASPET Journals on April 18, 2024

Molecular Pharmacology Fast Forward. Published on November 24, 2014 as DOI: 10.1124/mol.114.094979
This article has not been copyedited and formatted. The final version may differ from this version.

References

Balsalobre A, Marcacci L, and Schibler U (2000a) Multiple signaling pathways elicit circadian gene expression in cultured Rat-1 fibroblasts. *Curr Biol*, **10**: 1291–1294.

Balsalobre A, Brown SA, Marcacci L, Tronche F, Kellendonk C. Reichardt HM, Schutz G, and Schibler U (2000b). Resetting of circadian time in peripheral tissues by glucocorticoid signaling. *Science* **289**: 2344–2347.

Bleasby K, Castle JC, Roberts CJ, Cheng C, Bailey WJ, Sina JF, Kulkarni AV, Hafey MJ, Evers R, Johnson JM, Ulrich RG, and Slatter JG (2006) Expression profiles of 50 xenobiotic transporter genes in humans and pre-clinical species: a resource for investigations into drug disposition. *Xenobiotica* **36**: 963-988.

Bookout AL, Jeong Y, Downes M, Yu RT, Evans RM, and Mangelsdorf DJ (2006) Anatomical profiling of nuclear receptor expression reveals a hierarchical transcriptional network. *Cell* **126**: 789-799.

Braissant O, Foufelle F, Scotto C, Dauca M, and Wahli W (1996) Differential expression of peroxisome proliferator-activated receptors (PPARs): tissue distribution of PPAR-alpha, -beta, and -gamma in the adult rat. *Endocrinol* **137**:354-366.

Dreyer C, Krey G, Keller H, Givel F, Helftenbein G, and Wahli W (1992) Control of the peroxisomal β-oxidation pathway by a novel family of nuclear hormone receptors. *Cell* **68**: 879-887.

Gachon F, Olela FF, Schaad O, Descombes P, and Schibler U (2006) The circadian PAR-domain basic leucine zipper transcription factors DBP, TEF, and HLF modulate basal and inducible xenobiotic detoxification. *Cell metab* **4**: 25-36.

Gekakis N, Staknis D, Nguyen HB, Davis FC, Wilsbacher LD, King DP, Takahashi JS, and Weitz CJ (1998) Role of the CLOCK protein in the mammalian circadian mechanism. *Science* **280**: 1564-1569.

Hamdan AM, Koyanagi S, Wada E, Kusunose N, Murakami Y, Matsunaga N, and Ohdo S (2012) Intestinal expression of mouse Abcg2/Bcrp gene is under the control of circadian clock-activating transcription factor-4 pathway. *J Biol Chem* **287**:17224-17231.

Hrushesky WJ (2001) Tumor chronobiology. *J Control Release* **74**: 27-30.

Issemann I and Green S (1990) Activation of a member of the steroid hormone receptor superfamily by peroxisome proliferators. *Nature* **347**: 645-650.

Jin X, Shearman LP, Weaver DR, Zylka MJ, de Vries GJ, and Reppert SM (1999) A molecular mechanism regulating rhythmic output from the suprachiasmatic circadian

Downloaded from molpharm.aspetjournals.org at ASPET Journals on April 18, 2024

Molecular Pharmacology Fast Forward. Published on November 24, 2014 as DOI: 10.1124/mol.114.094979
This article has not been copyedited and formatted. The final version may differ from this version.

clock. *Cell* **96**: 57-68.

King DP, Zhao Y, Sangoram AM, Wilsbacher LD, Tanaka M, Antoch MP, Steeves TD, Vitaterna MH, Kornhauser JM, Lowrey PL, Turek FW, and Takahashi JS (1997) Positional cloning of the mouse circadian clock gene. *Cell* **89**: 641-653.

Kume K, Zylka MJ, Sriram S, Shearman LP, Weaver DR, Jin X, Maywood ES, Hastings MH, and Reppert SM (1999) mCRY1 and mCRY2 are essential components of the negative limb of the circadian clock feedback loop. *Cell* **98**: 193-206.

Lee Y, Yu X, Gonzales F, Mangelsdorf DJ, Wang MY, Richardson C, Witters LA, and Unger RH (2002) PPARα is necessary for the lipopenic action of hyperleptinemia on white adipose and liver tissue. *Proc Natl Acad Sci USA* **99**: 11848-11853.

Lefebvre P, Chinetti G, Fruchart J, and Staels B (2006) Sorting out the roles of PPARα in energy metabolism and vascular homeostasis. *J Clin Invest* **116**: 571-580.

Lévi F (1996) Chronopharmacology and chronotherapy of cancers. *Pathol Biol* **44**: 631-644.

Lis CG, Grutsch JF, Wood P, You M, Rich I, and Hrushesky WJ (2003) Circadian timing in cancer treatment: the biological foundation for an integrative approach. *Integr Cancer Ther* **2**: 105-111.

Maemura K, de la Monte SM, Chin MT, Layne MD, Hsieh CM, Yet SF, Perrella MA, and Lee ME (2000) CLIF, a novel cycle-like factor, regulates the circadian oscillation of plasminogen activator inhibitor-1 gene expression. *J Biol Chem* **275**: 36847-36851.

Motojima K, Passilly P, Peters JM, Gonzalez FJ, and Latruffe N (1998) Expression of putative fatty acid transporter genes are regulated by peroxisome proliferator-activated receptor α and γ activators in a tissue-and inducer-specific manner. *J Biol Chem* **273**: 16710-16714.

Murakami Y, Higashi Y, Matsunaga N, Koyanagi S, and Ohdo S (2008) Circadian clock-controlled intestinal expression of the multidrug-resistance gene mdr1a in mice. *Gastroenterology* **135**: 1636-1644.

Okamura A, Koyanagi S, Dilxiat A, Kusunose N, Matsunaga N, Shibata S, and Ohdo S. (2014) Bile acid-regulated PPARα activity underlies circadian expression of intestinal peptide absorption transporter PepT1/Slc15a1 *J Biol Chem* **289**: 25296-25305.

Ohdo S (2007) Chronopharmacology focused on biological clock. *Drug Metab Pharmacokinet* **22**: 3-14.

Oishi K, Miyazaki K, Kadota K, Kikuno R, Nagase T, Atsumi G, Ohkura N, Azama T, Mesaki M, Yukimasa S, Kobayashi H, Iitaka C, Umehara T, Horikoshi M, Kudo T,

Downloaded from molpharm.aspetjournals.org at ASPET Journals on April 18, 2024

Molecular Pharmacology Fast Forward. Published on November 24, 2014 as DOI: 10.1124/mol.114.094979
This article has not been copyedited and formatted. The final version may differ from this version.

Shimizu Y, Yano M, Monden M, Machida K, Matsuda J, Horie S, Todo T, and Ishida N. (2003) Genome-wide expression analysis of mouse liver reveals CLOCK-regulated circadian output genes. *J Biol Chem* 278: 41519-41527.

Oishi K, Amagai N, Shirai H, Kadota K, Ohkura N, and Ishida N (2005) Genome-wide expression analysis reveals 100 adrenal gland-dependent circadian genes in the mouse liver. *DNA Res* **12**: 191–202.

Preitner N, Damiola F, Lopez-Molina L, Zakany J, Duboule D, Albrecht U, and Schibler U (2002) The orphan nuclear receptor REV-ERBα controls circadian transcription within the positive limb of the mammalian circadian oscillator. *Cell* **110**: 251-260.

Ripperger JA, Shearman LP, Reppert SM, and Schibler U (2000) CLOCK, an essential pacemaker component, controls expression of the circadian transcription factor DBP. *Genes Dev* **14**: 679-689.

Ritskes-Hoitinga M (2004) Nutrition of laboratory mice. *The laboratory mouse* **1**, 463-479.

Sinal CJ, Yoon M, and Gonzalez FJ (2001) Antagonism of the actions of peroxisome proliferator-activated receptor-α by bile acids. *J Biol Chem* **276**: 47154-47162.

Stearns AT, Balakrishnan A, Rhoads DB, Ashley SW, and Tavakkolizadeh A (2008) Diurnal rhythmicity in the transcription of jejunal drug transporters. *J Pharmacol Sci* **108**: 144-148.

Tamai I, Ohashi R, Nezu JI, Sai Y, Kobayashi D, and Oku A (2000) Shimane M, Tsuji A. Molecular and functional characterization of organic cation/carnitine transporter family in mice. *J Biol Chem* **275**: 40064-40072.

Tamai I, Yabuuchi H, Nezu J, Sai Y, Oku A, Shimane M, and Tsuji A (1997) Cloning and characterization of a novel human pH-dependent organic cation transporter, OCTN1. *FEBS Lett* **419**, 107-111.

Terazono H, Mutoh T, Yamaguchi S, Kobayashi M, Akiyama M, Udo R, Ohdo S, Okamura H, and Shibata S. (2003) Adrenergic regulation of clock gene expression in mouse liver *Proc Natl.Acad Sci.USA* **100**: 6795–6800.

Tsuji A and Tamai I (1996) Carrier-mediated intestinal transport of drugs. *Pharm Res* **13**: 963-977.

Urban TJ, Brown C, Castro RA, Shah N, Mercer R, Huang Y, Brett CM, Burchard EG, and Giacomini KM (2007) Effects of genetic variation in the novel organic cation transporter, OCTN1, on the renal clearance of gabapentin. *Clin Pharmacol Ther* **83**: 416-421.

Downloaded from molpharm.aspetjournals.org at ASPET Journals on April 18, 2024

Molecular Pharmacology Fast Forward. Published on November 24, 2014 as DOI: 10.1124/mol.114.094979
This article has not been copyedited and formatted. The final version may differ from this version.

Vu-Dac N, Schoonjans K, Kosykh V, Dallongeville J, Fruchart JC, Staels B, and Auwerx J (1995) Fibrates increase human apolipoprotein A-II expression through activation of the peroxisome proliferator-activated receptor. *J Clin Invest* **96**: 741-750.

Wu X, Prasad PD, Leibach FH, and Ganapathy V (1998) cDNA sequence, transport function, and genomic organization of human OCTN2, a new member of the organic cation transporter family. *Biochem Biophys Res Commun* **46**: 589-59 (1998).

Yoo SH, Ko CH, Lowrey PL, Buhr ED, Song EJ, Chang S, Yoo OJ, Yamazaki S, Lee C, and Takahashi JS (2005) A noncanonical E-box enhancer drives mouse Period2 circadian oscillations in vivo. *Proc Natl Acad Sci U S A* **102**: 2608-2613.

Downloaded from molpharm.aspetjournals.org at ASPET Journals on April 18, 2024

Molecular Pharmacology Fast Forward. Published on November 24, 2014 as DOI: 10.1124/mol.114.094979
This article has not been copyedited and formatted. The final version may differ from this version.

Footnotes

This work was supported by a Grant-in-Aid for Scientific Research on Innovative Areas [25136716 to S.O.]; a Grant-in-Aid for Scientific Research (A) [25253038 to S.O.]; a Grant-in-Aid for Challenging Exploratory Research [25670079 to S.O.; 26670317 to S.K.] from the Japan Society for the Promotion of Science.

Downloaded from molpharm.aspetjournals.org at ASPET Journals on April 18, 2024

Molecular Pharmacology Fast Forward. Published on November 24, 2014 as DOI: 10.1124/mol.114.094979
This article has not been copyedited and formatted. The final version may differ from this version.

Figure legends

Figure1 Bile acids repress the PPARα/RXRα-induced expression of *Slc22a4* in the intestinal epithelial cells. (A) The circle graph depicts the most highly represented categories of bile acid-dependent PPARα-regulated genes in the mouse intestinal epithelial cells. (B) Mutation of PPREs abrogates PPARα/RXRα-mediated transactivation of the mouse *Slc22a4* gene. Luciferase activities of wild-type *Slc22a4*-Luc and PPRE-mutated *Slc22a4*-Luc (PPRE m1 and PPRE m2) were assessed by co-transfecting with expression vector encoding PPARα and RXRα. (C) Immortalized epithelial cells, aMoS7 (left) and Caco-2 (right) were transfected with both PPARα and RXRα expression vectors. At 24-h after transfection, cholic acid (CA) was added into the media at final concentration of 100, 250, or 500 μM. Values shown are shown the mean ± S.E. of 3 samples. * $p<0.05$, significantly different from control (pcDNA) group. #; $p<0.05$, significantly different from the PPARα and RXRα- transfected cells without CA treatment.

Figure 2 Circadian expression of *Slc22a4* in the small intestinal of mice. (A) Temporal pattern of food intake by wild type and PPARα-null mice. (B) Temporal accumulation profiles of bile acids in the intestinal cells of wild type and PPARα-null mice. (C) Temporal expression profile of *Slc22a4* mRNA in the small intestine of wild type and PPARα-null mice. (D) Temporal expression profiles of PPARα and Octn1 protein in the small intestine of wild type and PPARα-null mice. For panel A-C, Values shown are the mean ± S.E. of 4-6 mice for all panels * $p<0.05$, significantly different from wild-type mice at the corresponding time point. For panel D, the band intensity of protein was normalized to Actin and converted to the ratio to maximal level of wild- type mice. The values are plotted in the photographs of immunoblot.

Figure 3 Periodic stimulation with bile acid induce an oscillation in the expression of *Slc22a4* in cultured aMoS7 cells. (*A*) Temporal mRNA expression profiles of *Per1, Per2*

Downloaded from molpharm.aspetjournals.org at ASPET Journals on April 18, 2024

Molecular Pharmacology Fast Forward. Published on November 24, 2014 as DOI: 10.1124/mol.114.094979
This article has not been copyedited and formatted. The final version may differ from this version.

(upper), and *Slc22a4* (lower) in aMoS7 cells whose circadian clock was synchronized by the treatment with 50% serum for 2 h. (*B*) Temporal mRNA expression profiles of *Per1*, *Per2* (upper), and *Slc22a4* (lower) in aMoS7 cells treated repetitively with500 μM cholic acid (CA) for 4 h. Values are shown the mean ± S.E. of 4-5 samples.

Figure 4 Down-regulation of Octn1 diminishes the uptake of gabapentin into aMoS7 cells. (A) Treatment of aMoS7 cells with 500 μM cholic acid (CA) for 4 h transiently decreases the protein levels of Octn1 and gabapentin incorporation. Upper panels show immunoblots of Octn1 protein after CA treatment. *$p<0.05$, significantly different from basal levels (indicated as 0). (B) aMoS7 cells were transfected with scrambled siRNA (*Control* siRNA) or specific siRNA against *Slc22a4* gene (*Slc22a4* siRNA). The protein levels of Octn1 and gabapentin incorporation were assessed at 48 h after transfection. Values are shown as means with S.E.of 3-4 samples. *$p<0.05$, significantly different from control siRNA-transfected group (indicated as 0). The band intensity was plotted by normalizing to Actin, and mean value of basal levels was set as 1.0. The values are plotted in the photographs of immunoblot.

Figure 5 Dosing time-dependent change in the pharmacokinetics of gabapentin after oral administration. (A) Time-dependency of [^{3}H]-gabapentin accumulation in the small intestine of wild-type mice. The jejunal segments were incubated with 5 μM [^{3}H]-gabapentin in the presence or absence of 10 mM tetraethylammonium (TEA) and/or non-radio-labeled (cold) gabapentin. Values are shown as means with S.E. of six mice. * $p < 0.05$ compared with the value for ZT2. (B) Wild-type mice were orally administered with gabapentin (65 mg/kg) at ZT2 (open circles) or ZT14 (closed circles)**.** Values are shown as means with S.E. of six mice. * $p < 0.05$ compared with the value for ZT2 administration.

Downloaded from molpharm.aspetjournals.org at ASPET Journals on April 18, 2024

Molecular Pharmacology Fast Forward. Published on November 24, 2014 as DOI: 10.1124/mol.114.094979
This article has not been copyedited and formatted. The final version may differ from this version.

Table 1 Influence of dosing times on pharmacokinetic parameters after the oral administration of gabapentin (65 mg/kg) at ZT2 or ZT14.

Pharmacokinetic parameters	Time of drug administration		Significance
	ZT2	ZT14	
CL/F (L/h/kg)	2.199 ± 0.009	2.150 ± 0.016	N.S.
Vd (L/kg)	0.659 ± 0.012	0.613 ± 0.011	N.S.
AUC (μg. h/mL)	29.569 ± 0.118	30.268 ± 0.227	N.S.
ka (/hr)	0.976 ± 0.080	1.686 ± 0.122	$p<0.01$
$t_{1/2}$ (hr)	0.208 ± 0.005	0.198 ± 0.004	N.S.

Values are the mean ± S.E. of 39 mice. Significant differences between the two groups were evaluated by the Student's *t*-test. The 1% level of probability was considered to be significant. N.S., not significant.

Downloaded from molpharm.aspetjournals.org at ASPET Journals on April 18, 2024

Molecular Pharmacology Fast Forward. Published on November 24, 2014 as DOI: 10.1124/mol.114.094979
This article has not been copyedited and formatted. The final version may differ from this version.

Figure 1

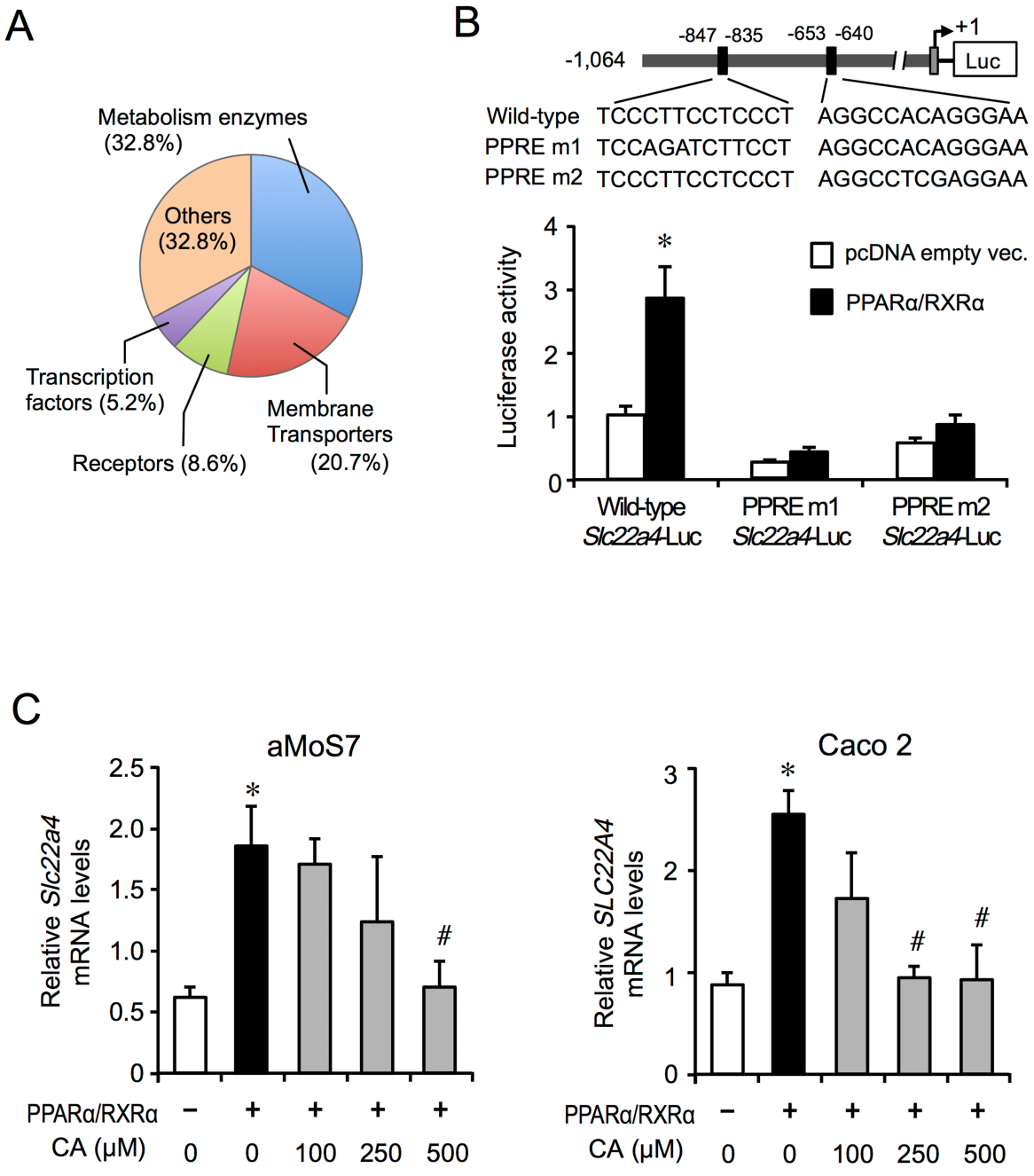

Molecular Pharmacology Fast Forward. Published on November 24, 2014 as DOI: 10.1124/mol.114.094979
This article has not been copyedited and formatted. The final version may differ from this version.

Figure 2

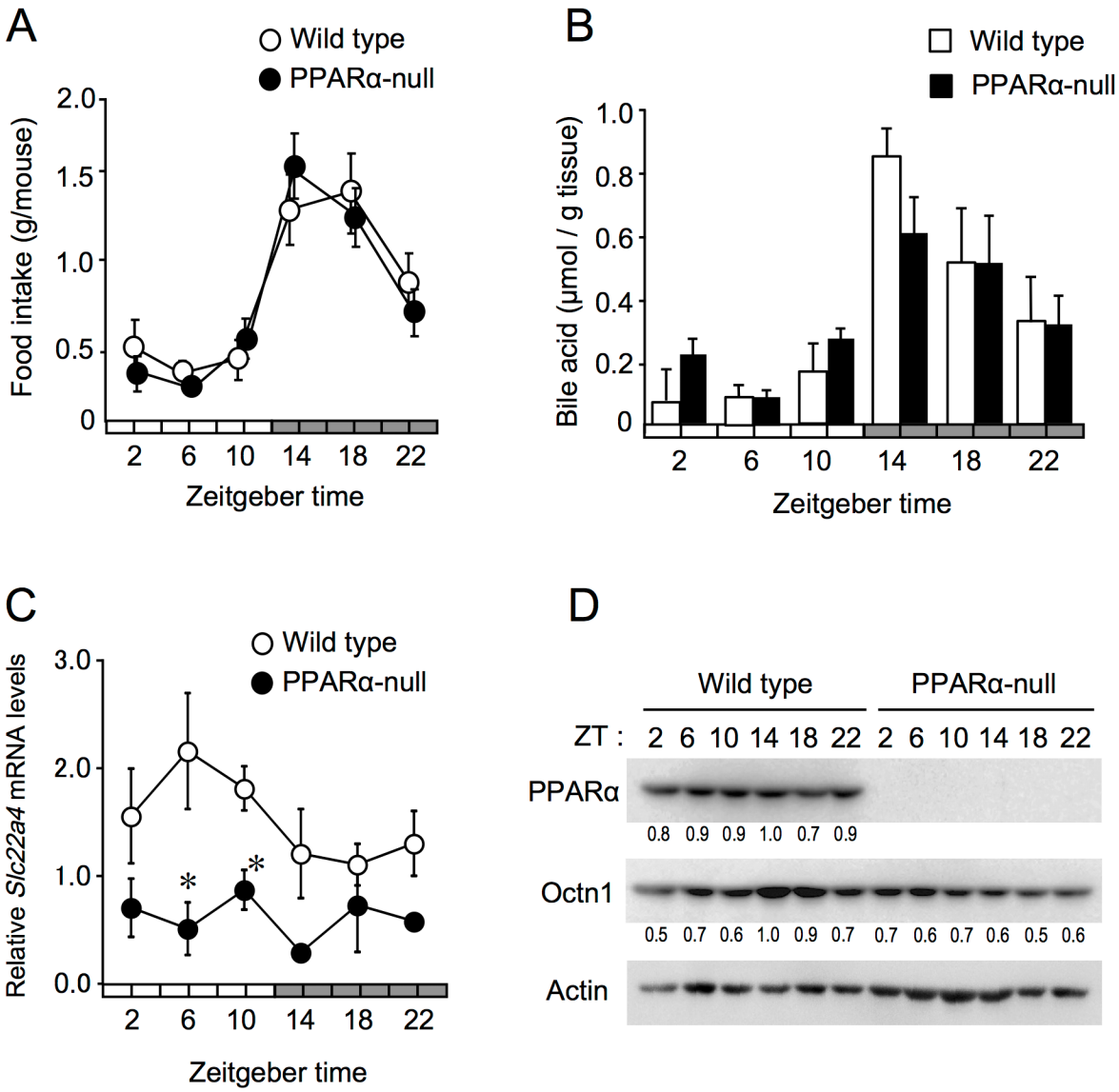

Molecular Pharmacology Fast Forward. Published on November 24, 2014 as DOI: 10.1124/mol.114.094979
This article has not been copyedited and formatted. The final version may differ from this version.

Figure 3

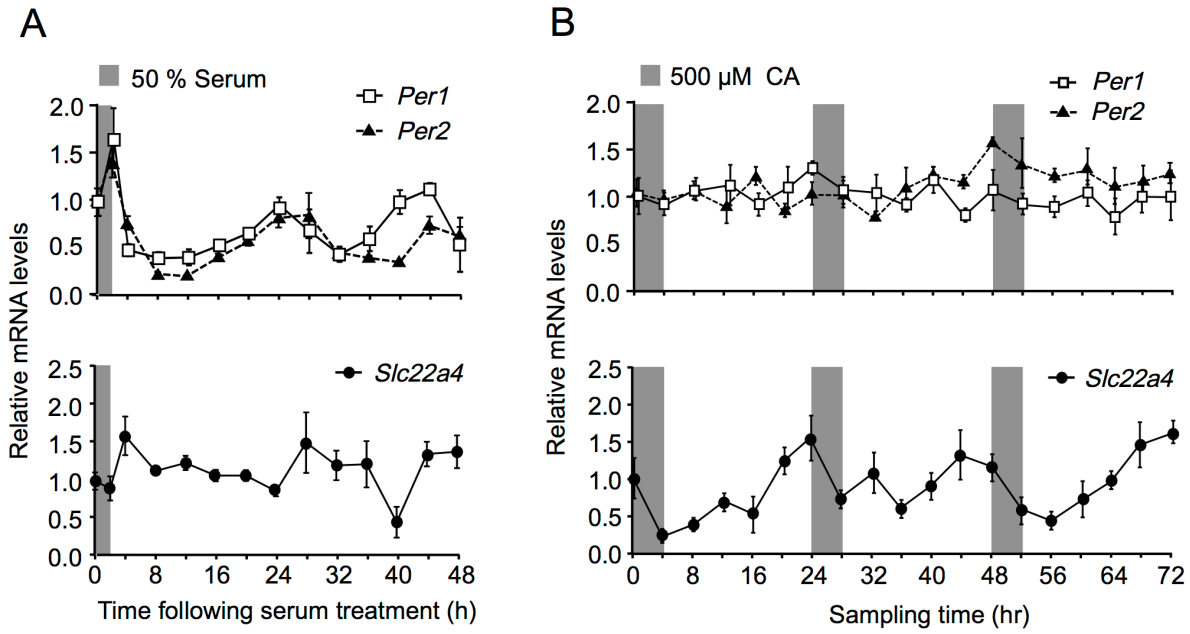

Molecular Pharmacology Fast Forward. Published on November 24, 2014 as DOI: 10.1124/mol.114.094979
This article has not been copyedited and formatted. The final version may differ from this version.

Figure 4

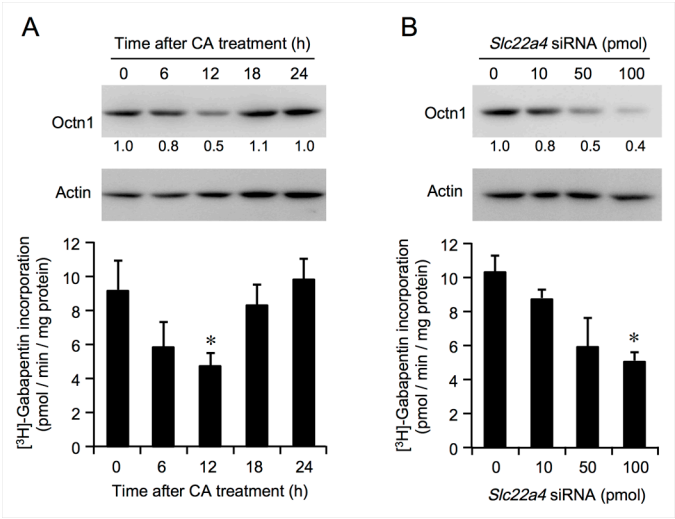

Molecular Pharmacology Fast Forward. Published on November 24, 2014 as DOI: 10.1124/mol.114.094979
This article has not been copyedited and formatted. The final version may differ from this version.

Figure 5

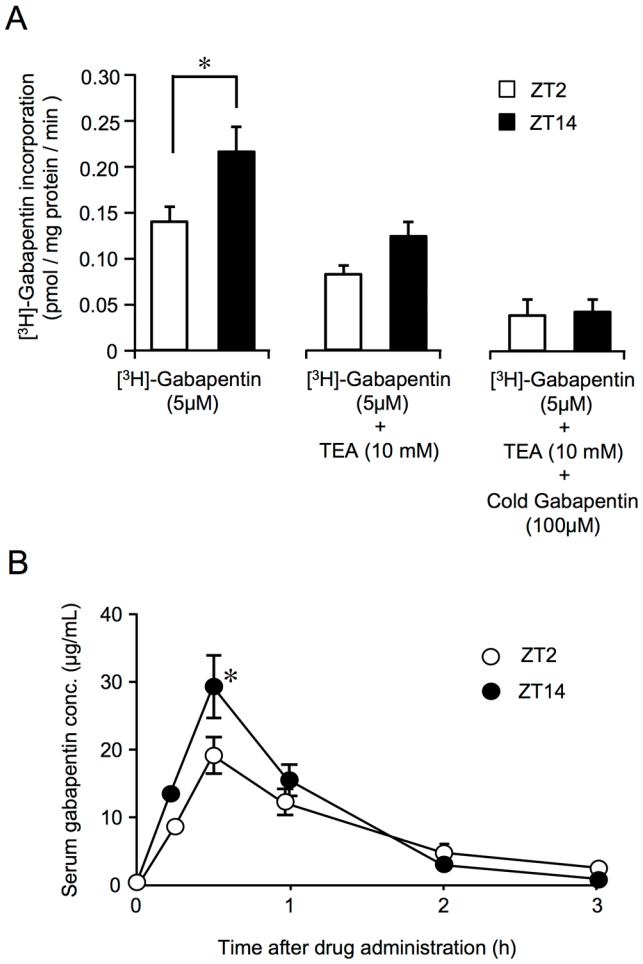

Modulation of PPARα activity by bile acids causes circadian changes in the intestinal expression of Octn1/Slc22a4 in mice
Wada E, Koyanagi S, Kusunose N, Akamine T, Masui H, Hashimoto H, Matsunaga N, and Ohdo S
Molecular Pharmacology

Supplemental Table S1 Candidates for bile acid-dependent PPARα-target genes in the mouse intestinal cells

Entrez gene ID	Unigene ID	Gene symbol	Gene description	Chromosome	Wild-type CA / Wild-type veh.	Z-score
18780	Mm.4675	Pla2g2a	phospholipase A2, group IIA	4	0.0415	-5.7886
20393	Mm.28405	Sgk1	serum glucocorticoid regulated kinase-1	10	0.1619	-5.2465
56221	Mm.31505	Ccl24	chemokine ligand 24	5	0.1488	-5.2170
209558	Mm.338425	Enpp3	ectonucleotide pyrophosphatase/phosphodiesterase 3	10	0.2572	-3.9997
30805	Mm.274590	Slc22a4	solute carrier family 22 (organic cation transporter), member 4	11	0.2143	-3.9621
20250	Mm.487021	Scd2	stearoyl-Coenzyme A desaturase 2	19	0.1860	-3.9510
13162	Mm.41993	Slc6a3	solute carrier family 6 (neurotransmitter transporter, dopamine), member 3	13	0.1143	-3.9476
20787	Mm.278701	Srebf1	sterol regulatory element binding transcription factor 1	11	0.3030	-3.5193
56643	Mm.155618	Slc15a1	solute carrier family 15 (oligopeptide transporter), member 1	14	0.2971	-3.4941
17748	Mm.192991	Mt1	NOD-derived CD11c +ve dendritic cells	8	0.1469	-3.4924
11807	Mm.389209	Apoa2	apolipoprotein A-II テキスト	1	0.2968	-3.3279
23959	Mm.244235	Nt5e	5' nucleotidase	9	0.3395	-3.1082
20778	Mm.282242	Scarb1	scavenger receptor class B, member 1	5	0.1838	-3.0846
116914	Mm.35444	Slc19a2	solute carrier family 19 (thiamine transporter), member 2	1	0.3446	-3.0658
246228	Mm.26515	Vwa1	von Willebrand factor A domain containing 1	4	0.3538	-2.9897
11430	Mm.356689	Acox1	acyl-CoA oxidase	11	0.3637	-2.9097
57279	Mm.29666	Slc25a20	solute carrier family 25 (mitochondrial carnitine/acylcarnitine translocase), member 20	9	0.3767	-2.8085
54338	Mm.103581	Slc23a2	solute carrier family 23 (nucleobase transporters), member 2	2	0.3594	-2.8045
14667	Mm.287807	Gm2a	GM2 ganglioside activator protein	11	0.0486	-2.7705
50934	Mm.276831	Slc7a8	solute carrier family 7 (cationic amino acid transporter, y+ system), member 8	14	0.3831	-2.7596
12521	Mm.4261	Cd82	CD82 antigen	2	0.4824	-2.6184
30805	Mm.474216	Cyp2d22	cytochrome P450, family 2, subfamily d, polypeptide 22	15	0.3314	-2.5933
230857	Mm.401062	Ece1	endothelin converting enzyme 1	4	0.2434	-2.5742
15959	Mm.426079	Ifit3	interferon-induced protein with tetratricopeptide repeats 3	19	0.3397	-2.5347
26876	Mm.158750	Adh4	alcohol dehydrogenase 4	3	0.3442	-2.5044
13649	Mm.8534	Egfr	epidermal growth factor receptor	11	0.4011	-2.5040
64385	Mm.486449	Cyp4f14	cytochrome P450, family 4, subfamily f, polypeptide 14	17	0.4258	-2.4879
14114	Mm.297992	Fbln1	fibulin 1	15	0.3472	-2.4836
20520	Mm. 42253	Slc22a5	solute carrier family 22 (organic anion transporter), member 5	11	0.3483	-2.4761
77128	Mm.275414	Crebrf	CREB3 regulatory factor	17	0.2579	-2.4689
15007	Mm.88795	H2-Q10	histocompatibility 2, Q region locus 10	17	0.4267	-2.4484
17750	Mm.147226	Mt2	metallothionein 2	8	0.4437	-2.4000
13117	Mm.10742	Cyp4a10	cytochrome P450, family 4, subfamily a, polypeptide 10	4	0.4393	-2.3645
12491	Mm.18628	Cd36	CD36 antigen (fattry acid translocase)	5	0.4243	-2.3504
19299	Mm.399042	Abcd3	ATP-binding cassette, sub-family D (ALD), member 3	3	0.4421	-2.3465
26367	Mm.439731	Ceacam2	carcinoembryonic antigen-related cell adhesion molecule 2	7	0.4522	-2.3446
233836	Mm.211838	Slc5a11	solute carrier family 5 (sodium/glucose cotransporter), member 11	7	0.3234	-2.3309
54396	Mm.458517	Irgm2	immunity-related GTPase family M member 2	11	0.4277	-2.3286
14969	Mm.22564	H2-Eb1	histocompatibility 2, class II antigen E beta	17	0.4576	-2.3096
13850	Mm.15295	Ephx2	epoxide hydrolase 2	14	0.4596	-2.2970
170716	Mm.254838	Cyp4f13	cytochrome P450, family 4, subfamily f, polypeptide 13	17	0.4498	-2.2964
105785	Mm.298199	Kdelr3	KDEL (Lys-Asp-Glu-Leu) endoplasmic reticulum protein retention receptor 3	15	0.3852	-2.2395
16438	Mm.227912	Itpr1	inositol 1,4,5-trisphosphate receptor 1	6	0.3876	-2.2247
12660	Mm.225505	Chka	choline kinase alpha	19	0.2806	-2.1999
16889	Mm.157545	Lipa	lysosomal acid lipase A	19	0.4511	-2.1828
13666	Mm.247167	Eif2ak3	eukaryotic translation initiation factor 2 alpha kinase 3	6	0.4518	-2.1783
72303	Mm.482578	Cyp2c65	cytochrome P450, family 2, subfamily c, polypeptide 65	19	0.4686	-2.1782
19146	Mm.5184	Tmprss15	transmembrane protease, serine 15	16	0.0945	-2.1637
14311	Mm.10026	Cidec	cell death-inducing DFFA-like effector c	6	0.4552	-2.1578
11522	Mm.2409	Adh1	alcohol dehydrogenase 1	3	0.4758	-2.1345
26458	Mm.290044	Slc27a2	solute carrier family 27, member 2	2	0.4824	-2.0943
65969	Mm.313915	Cubn	intrinsic factor-cobalamin receptor	2	0.4099	-2.0930
269346	Mm.29510	Slc28a2	solute carrier family 28 (sodium-coupled nucleoside transporter), member 2	2	0.4927	-2.0926
72361	Mm.26580	Ces2g	carboxylesterase 2G	8	0.3188	-2.0838
15200	Mm.289681	Hbegf	heparin-binding EGF-like growth factor	18	0.4903	-2.0474
20517	Mm.594	Slc22a1	solute carrier family 22 (organic cation transporter), member 1	17	0.4800	-2.0125
19719	Mm.871	Rfng	RFNG O-fucosylpeptide 3-beta-N-acetylglucosaminyltransferase	11	0.4972	-2.0074
100494	Mm.24521	Zfand2a	zinc finger, AN1-type domain 2A	5	0.4819	-2.0018